Original Research Paper

Volume - 12 | Issue - 08 | August - 2022 | PRINT ISSN No. 2249 - 555X | DOI : 10.36106/ijar

Radiodiagnosis

CONVENTIONAL MRI FINDINGS IN NORMAL PRESSURE HYDROCEPHALUS.

Dr. Sehrish Shaheen*	MD, Department of Radiodiagnosis and Imaging, SKIMS, Soura, Srinagar, Jammu & Kashmir *Corresponding Author
Prof. Feroze Shaheen	MD, Department of Radiodiagnosis and Imaging, SKIMS, Soura, Srinagar, Jammu & Kashmir
Dr. Umar Nazir	MD, Department of Radiodiagnosis and Imaging, SKIMS, Soura, Srinagar, Jammu & Kashmir
Dr. Shumyla Jabeen	MD, DM, Department of Radiodiagnosis and Imaging, SKIMS, Soura, Srinagar, Jammu & Kashmir
Prof. Tariq Gojwari	MD, Department of Radiodiagnosis and Imaging, SKIMS, Soura, Srinagar, Jammu & Kashmir
Dr. Sajad Arif	Mch, Department of Neurosurgery, SKIMS, Soura, Srinagar, Jammu & Kashmir

ABSTRACT **Background:** Differentiation of NPH from other neurodegenerative diseases is challenging due to overlapping clinical & imaging features. This study aims to demonstrate various conventional MRI findings in clinically suspected patients of NPH. **Methods:** The study group comprised 36 patients and 10 asymptomatic age-matched controls. They were assessed on MRI for Evans' index, callosal angle, Sylvian fissure width, third ventricle diameter, temporal horn of lateral ventricle diameter, deep white matter hyperintensities, & aqueductal flow void. **Results:** In controls & cases respectively, Evans' index was 0.26 ± 0.02 & 0.34 ± 0.04, callosal angle was 104.5 ± 5.5° & 84.0 ± 8.7°, Sylvian fissure width was 3.2 ± 0.9 mm & 6.5 ± 1.4 mm, third ventricle diameter was 5.8 ± 1.3 mm & 12.7 ± 2.6 mm, & temporal horn diameter was 3.9 ± 0.9 mm & 7.4 ± 2.3 mm. Percentages of controls & cases with various grades of DWMH were similar. Aqueductal flow void was seen in 94.4% of cases & none of the controls. **Conclusion:** NPH patients have higher Evans' index, smaller callosal angle, wide Sylvian fissures, dilated third ventricle & temporal horns compared to controls. CSF flow void is exclusively seen in cases. There is no difference in DWMH between cases and controls.

KEYWORDS : Normal Pressure Hydrocephalus, MRI

INTRODUCTION

Diagnosis of Normal Pressure Hydrocephalus is challenging. Beyond the clinical features such as the classically described triad of gait disturbance, urinary incontinence, and memory impairment, there is a lack of a "gold standard" test to confirm the clinical diagnosis of NPH.[1] Many diagnostic measures for NPH, such as the measurement of CSF pressure, intrathecal saline infusion test, intermittent CSF drainage, measurement of the cerebral blood flow, and even brain biopsy, have been suggested in the literature[2-6] Radionuclide cisternography, computerized tomography, magnetic resonance imaging, CT cisternography, phase-contrast MRI, and perfusion MRI are among the imaging techniques used in the diagnosis of NPH[2, 5, 6] However, all diagnostic workup described yield false-positive and false-negative results. Differential diagnosis of NPH from other types of dementia is important as CSF diversion in the former may lead to clinical improvement.[5-7] However, clinical response to shunt surgery is highly variable.[6, 7] Additionally, the surgical treatment carries with it significant short- and long- term risks, and the etiopathogenesis of many NPH cases is unknown[5] Inspite of extensive research, an objective method of diagnosing NPH and predicting response to treatment remains elusive.[2, 5-7] Intracranial pressure (ICP) monitoring and cerebrospinal fluid (CSF) infusion tests are invasive and costly. Their reliability and reproducibility are also limited.[7] MRI poses an attractive alternative to these tests because of its non-invasive nature. In addition, unlike CT, it is non-ionising and is highly suited as a research tool.

MATERIALS AND METHODS

The study was conducted at a tertiary care institute in North India over a period of two years.

A total of 36 patients and 10 controls were included in the study.

Detailed informed consent was taken from the patients and controls before inclusion in the study.

Study Design: Prospective study

Selection of subjects:

Inclusion Criteria:

1. All patients clinically suspected of NPH i.e., presence of one or more symptoms of the triad
2. Age ≥ 60 years

Exclusion Criteria:

1. Age < 60 years
2. Obstructive hydrocephalus
3. Dementias other than NPH that could cause similar clinical symptoms or radiological findings
4. History or evidence of conditions that might cause secondary NPH
5. Patients with general contraindications to MRI

All Magnetic Resonance Imaging (MRI) studies were performed using a 1.5 Tesla MR system (Magnetom Avanto, Siemens Medical Systems, Erlangen, Germany), with a standard head coil, in neutral supine position.

The following protocol was used:

Table 1: MRI protocol

Sequence	FOV (mm/%)	Slice thickness (mm)	TR/TE (ms)	NEX	Flip angle (degrees)
t1_tse_tra	230/90	5	450/10	1	90
t2_tse_tra	230/91.1	5	3500/110	1	150
t2_tirm_tra_dark-fluid	230/87.5	5	9000/97	2	150
t2_spc_sag	256/100	0.82	1400/104	1	150

FOV = field of view, TR = time to repeat, TE = time to echo, NEX = number of excitations, tse = turbo spin echo, tra = transverse axial, tirm = turbo inversion recovery magnitude, spc = space, sag = sagittal, mm = millimetre , ms = millisecond

All suspected NPH patients were assessed on routine MRI for:

1. *Evans' index (EI):*

The maximum width of the frontal horns of the lateral ventricles and the maximum internal diameter of the skull at the same level on axial images were obtained and their ratio was taken as EI.

2. *Callosal angle (CA):*

A sagittal image was used to identify the anterior/posterior commissure plane and the posterior commissure. The CA was measured as the angle between the lateral ventricles on a coronal image through the posterior commissure, perpendicular to the AC/PC plane (using the capability to re-angle in the PACS).

3. *Width of Sylvian fissure:*

Measured in millimetres on a sagittal image located at the midpoint between the skull and the insular cortex, in five different locations perpendicular to the direction of the Sylvian fissure. The median value of the five locations was calculated for each side, and the average of right and left was recorded.

4. *Diameter of third ventricle:*

Measured in millimetres on axial images in the widest part.

5. *Diameter of temporal horn of lateral ventricle:*

Measured in millimetres on both sides on axial images and the mean of left and right sides was calculated.

6. *Deep white matter hyperintensities (DWMH):*

Evaluated on T2/FLAIR images and graded by the ordinal scale described by Fazekas et al. as follows[8]: 0 - no lesions, 1 - punctate foci, 2 - beginning confluence of foci, 3 - large confluent areas.

7. *Extent of flow void through the aqueduct and fourth ventricle:*

Observed on T2 sagittal images and graded by a modified version of the ordinal scale described by Algin et al. as follows[9]: 0 - no flow void in the aqueduct, 1 - flow void only in the aqueduct, 2 - flow void in the aqueduct and the upper half of the fourth ventricle, 3- flow void that extends to the caudal part of the fourth ventricle. all of the above includes all 1-7 values.

Statistical Analysis:

Data obtained was entered into Microsoft Excel Spreadsheets. Categorical variables were summarized as frequency and percentage. Continuous variables were summarized as mean and standard deviation and represented as Box plots showing mean (x), 25th, median and 75th percentiles (box) and ±95th percentiles (whiskers). A two-sided p-value was reported, and a p-value of < 0.05 was considered statistically significant.

OBSERVATIONS AND RESULTS

There were 36 patients of NPH and 10 age-matched controls.

Table 2: Comparison of Evans' index in controls and cases		
Controls	Cases	P-value
0.26 ± 0.02	0.34 ± 0.04	0.00001

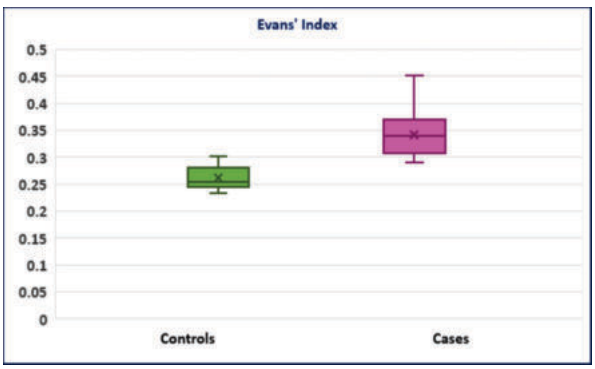

Figure 1. *Box plots showing the comparison of Evans' index in controls and cases*

Table 3: Comparison of callosal angle in controls and cases		
Controls	Cases	P-value
104.5 ± 5.5°	84.0 ± 8.7°	0.00001

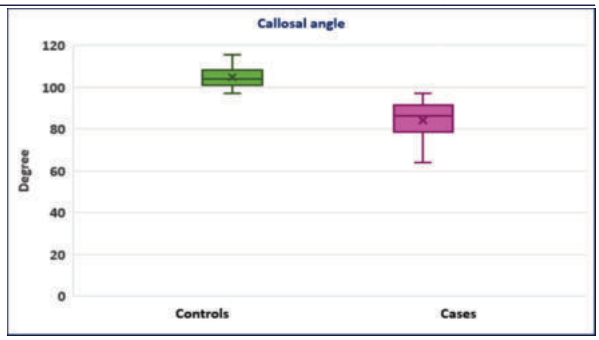

Figure 2. *Box plots showing the comparison of callosal angle in controls and cases*

Table 4: Comparison of width of Sylvian fissure in controls and cases		
Controls	Cases	P-value
3.2 ± 0.9 mm	6.5 ± 1.4 mm	0.00001

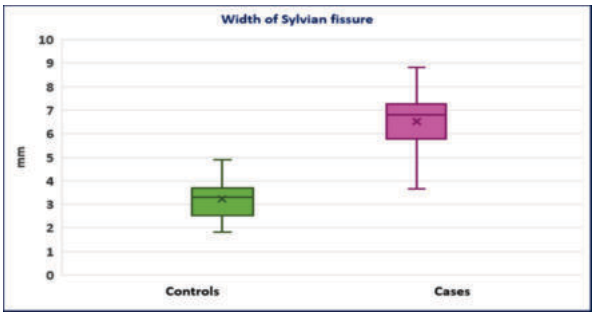

Figure 3. *Box plots showing the comparison of width of Sylvian fissure in controls and cases*

Table 5: Comparison of diameter of third ventricle in controls and cases		
Controls	Cases	P-value
5.8 ± 1.3 mm	12.7 ± 2.6 mm	0.00001

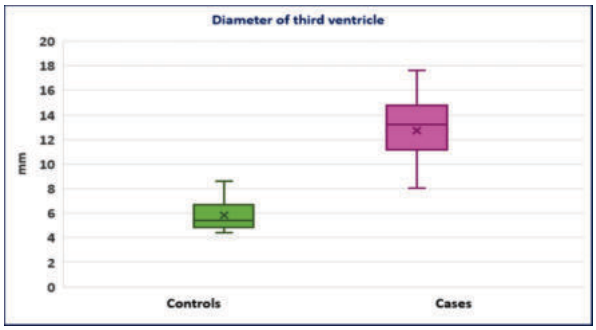

Figure 4. *Box plots showing the comparison of diameter of third ventricle in controls and cases*

Table 6: Comparison of diameter of temporal horn of lateral ventricle in controls and cases		
Controls	Cases	P-value
3.9 ± 0.9 mm	7.4 ± 2.3 mm	0.00001

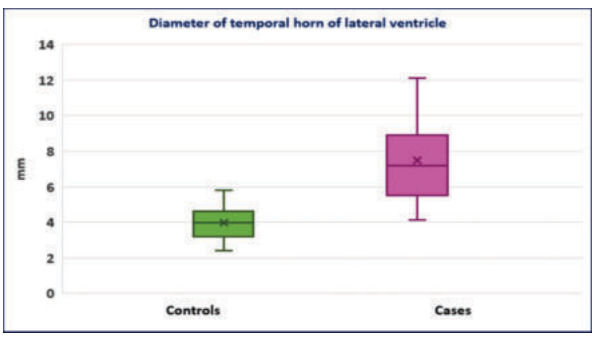

Figure 5. *Box plots showing the comparison of diameter of temporal horn of lateral ventricle in controls and cases*

Table 7: Comparison of deep white matter hyperintensities in controls and cases

Grade	Controls		Cases		p-value
	Number	Percentage	Number	Percentage	
0	1	10	3	8.3	0.42
1	1	10	5	13.9	
2	3	30	9	25	
3	5	50	19	52.8	

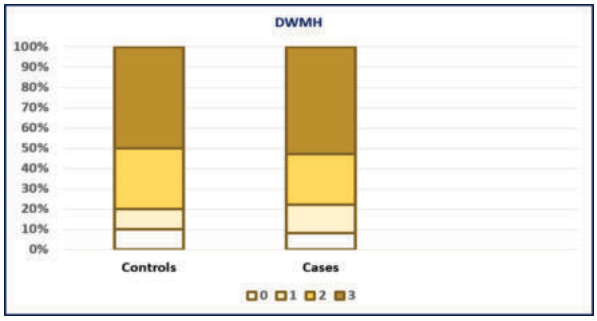

Figure 6. *Stacked columns showing the comparison of deep white matter hyperintensities in controls and cases*

Table 8: Comparison of flow void through the aqueduct and fourth ventricle in controls and cases

Grade	Controls		Cases	
	Number	Percentage	Number	Percentage
0	10	100	2	5.6
1	0	0	0	0
2	0	0	8	22.2
3	0	0	26	72.2

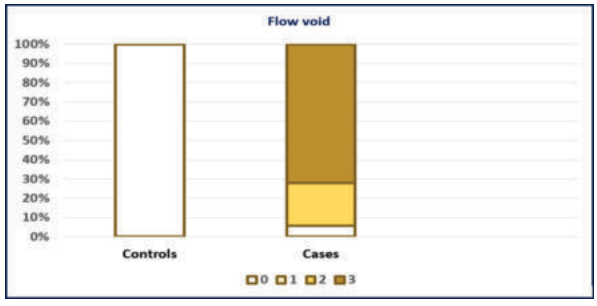

Figure 7. *Stacked columns showing the comparison of flow void through the aqueduct and fourth ventricle in controls and cases*

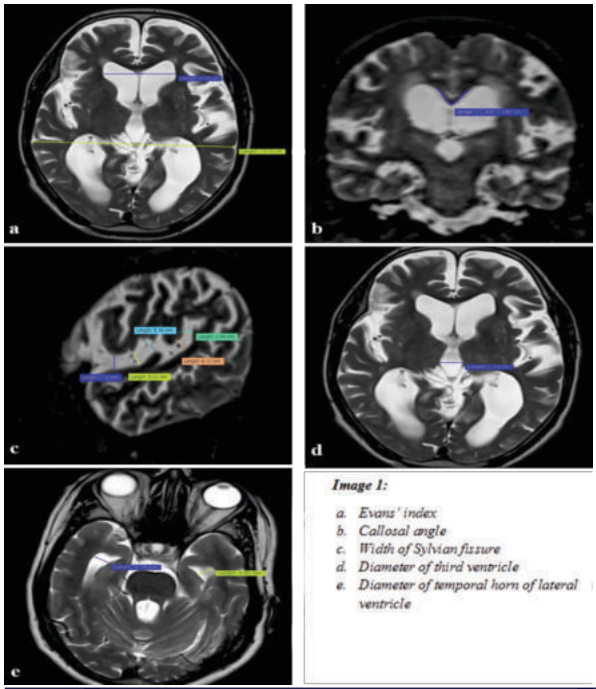

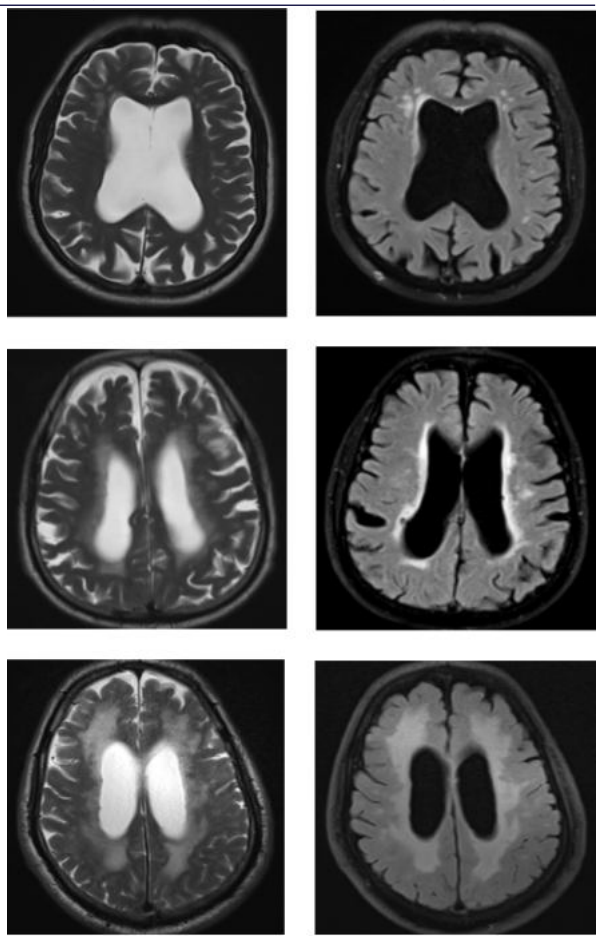

Image 2: *T2 & FLAIR axial images showing Grade 1, 2 & 3 DWMH.*

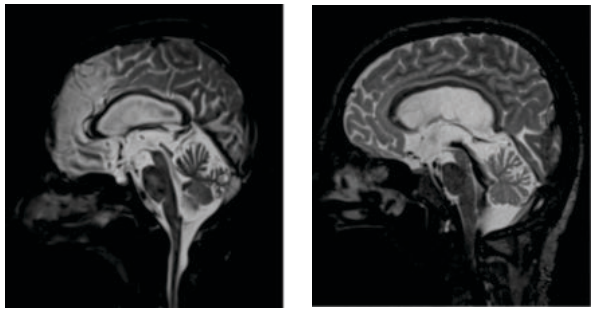

Image 3: *T2 space sagittal images showing Grade 2 & 3 CSF flow void.*

DISCUSSION

***Evans' index*:**

EI was higher in cases than controls, with a statistically significant difference (p-value < 0.05). This is in accordance with the literature-established definition of ventriculomegaly as EI of 0.3 or greater.[10]

Callosal angle:

CA was smaller in cases than in controls, with a statistically significant difference (p-value < 0.05). This corroborates the conventional usage of CA as a marker of NPH with a value of < 90°.[10] CA is mainly a marker of ventricular size. A small CA has previously been useful for separating patients with iNPH from those with Alzheimer's disease and healthy controls (Ishii K et al.).[11] Several authors have proposed a plausible theory to explain the small CA in hydrocephalus: the dilatation of the lateral ventricles elevates the corpus callosum until it reaches the level of the falx, while the lateral portions of the roof of the lateral ventricles continue to rise, thus decreasing the CA.[12]

Width of Sylvian fissure:

Sylvian fissures were wider in cases than in controls, with a statistically significant difference (p-value < 0.05). This was also found in a study

by Fallmar et al.[13], which described significantly enlarged Sylvian fissures in NPH. A communicating hydrocephalus with dilated ventricles and disproportionate distribution of the CSF between the superior and inferior subarachnoid spaces, i.e. compression of the medial/high convexity cortex sulci and dilation of the Sylvian fissures is referred to as DESH (Disproportionately Enlarged Subarachnoid space Hydrocephalus).[14] This was the highlight of a research paper from the Japanese Study of Idiopathic Normal Pressure Hydrocephalus on Neurological Improvement (SINPHONI) which described DESH as an imaging hallmark of iNPH.[14] In this study, widened Sylvian fissures were seen in about 96% of the patients and were classified as having DESH. In our study, the finding of only widened Sylvian fissures was evaluated and emphasised as an important finding in NPH.

Diameter of third ventricle:

Third ventricle was dilated in cases as compared to controls, with a statistically significant difference (p-value < 0.05). Increased diameter of the third ventricle in NPH has previously been seen in a study conducted by Virhammar et al.[15]

Diameter of temporal horn of lateral ventricle:

Temporal horns of lateral ventricles were dilated in cases as compared to controls, with a statistically significant difference (p-value < 0.05). Dilation of temporal horns of lateral ventricles is an established finding in hydrocephalus and was used as a parameter to differentiate NPH from cerebral atrophy by Tans JT et al.[16] This finding was strengthened by the results of our study. Dilatation of the temporal horns of the lateral ventricles is one of the earliest signs of hydrocephalus.[17]

Deep white matter hyperintensities:

We found no significant difference in DWMH between NPH patients and controls (p-value > 0.05). This correlates with the study by Fallmar et al.[13] which stated that there was no difference in DWMH between NPH patients and other groups, including healthy controls. DWMH is commonly associated with risk factors for vascular disease like hypertension and smoking. The origin of DWMH is still disputed. Various authors have reported these hyperintensities to represent chronic ischemia, gliosis or plasma leakage caused by diffuse cerebrovascular endothelial failure.[18] In NPH, it is the transependymal CSF passage into the adjacent white matter that probably causes the DWMH around the lateral ventricles .[19]

Flow void through the aqueduct and fourth ventricle:

On MR imaging, the CSF flow void via the cerebral aqueduct and fourth ventricle indicates hyperdynamic CSF flow akin to the flow voids seen in arteries.[20] Generally, the signal intensity of flowing fluid decreases as the flow velocity increases. As the fluid flows rapidly beyond a threshold, it loses its signal on MRI. This signal loss is termed the flow void phenomenon.[21] In our study, all controls had Grade 0 i.e. no flow void. Out of 36 cases, 2 (5.6 %) had Grade 0, 8 (22.2 %) had Grade 2 and 26 (72.2 %) had Grade 3 flow void. In our study, CSF flow void had a sensitivity of 94.44%, specificity of 100% and accuracy of 95.65% for NPH. Flow void in NPH was also ascertained in a study by Bradley et al.[22] which stated that while healthy individuals can exhibit aqueductal flow void, this phenomenon is most prominent in chronic communicating NPH patients, is less apparent in patients with acute communicating hydrocephalus and is least apparent in patients with brain atrophy. In NPH, ventricular enlargement pushes the brain parenchyma close to the cranium. During systole, blood flows into the cerebral hemispheres and since the brain cannot expand outwards, it expands only inwards. This inward expansion compresses the lateral and third ventricles, expelling a large volume of CSF via the aqueduct and this leads to a prominent CSF flow void.[22]

CONCLUSION

Conventional MRI findings in NPH patients include a higher Evans' index, a smaller callosal angle, wide Sylvian fissures, dilated third ventricle and dilated temporal horns of lateral ventricles, as compared to age-matched controls. CSF flow void through the aqueduct and fourth ventricle is seen in NPH patients but not in controls. There is no significant difference in deep white matter hyperintensities in NPH patients and age-matched controls.

Conflicts of interest: Nil

REFERENCES

1. Luetmer, P. H., Huston, J., Friedman, J. A., Dixon, G. R., Petersen, R. C., Jack, C. R., McClelland, R. L., & Ebersold, M. J. (2002). Measurement of cerebrospinal fluid flow at the cerebral aqueduct by use of phase-contrast magnetic resonance imaging: technique validation and utility in diagnosing idiopathic normal pressure hydrocephalus. Neurosurgery, 50(3), 534–544. https://doi.org/10.1097/00006123-200203000-00020
2. Algin O. (2010). Role of aqueductal CSF stroke volume in idiopathic normal-pressure hydrocephalus. AJNR. American journal of neuroradiology, 31(2), E26–E28. https://doi.org/10.3174/ajnr.A1943
3. Holodny, A. I., Waxman, R., George, A. E., Rusinek, H., Kalnin, A. J., & de Leon, M. (1998). MR differential diagnosis of normal-pressure hydrocephalus and Alzheimer disease: significance of perihippocampal fissures. AJNR. American journal of neuroradiology, 19(5), 813–819.
4. Brecknell, J. E., & Brown, J. I. (2004). Is idiopathic normal pressure hydrocephalus an independent entity?. Acta neurochirurgica, 146(9), 1003–1007. https://doi.org/10.1007/s00701-004-0332-2
5. Graff-Radford N. R. (2007). Normal pressure hydrocephalus. Neurologic clinics, 25(3), 809–viii. https://doi.org/10.1016/j.ncl.2007.03.004
6. Stein, S. C. (2001a). Normal-Pressure Hydrocephalus: An Update: Neurosurgery Quarterly, 11(1), 26–35. https://doi.org/10.1097/00013414-200103000-00004
7. Vanneste J. A. (2000). Diagnosis and management of normal-pressure hydrocephalus. Journal of neurology, 247(1), 5–14. https://doi.org/10.1007/s004150050003
8. Fazekas, F., Chawluk, J. B., Alavi, A., Hurtig, H. I., & Zimmerman, R. A. (1987). MR signal abnormalities at 1.5 T in Alzheimer's dementia and normal aging. AJR. American journal of roentgenology, 149(2), 351–356. https://doi.org/10.2214/ajr.149.2.351
9. Algin, O., Hakyemez, B., Taskapilioglu, O., Ocakoglu, G., Bekar, A., & Parlak, M. (2009). Morphologic features and flow void phenomenon in normal pressure hydrocephalus and other dementias: are they really significant?. Academic radiology, 16(11), 1373–1380. https://doi.org/10.1016/j.acra.2009.06.010
10. Evans, W. A. (1942). An encephalographic ratio for estimating ventricular enlargement and cerebral atrophy. Archives of Neurology And Psychiatry, 47(6), 931. https://doi.org/10.1001/archneurpsyc.1942.02290060069004
11. Ishii, K., Kanda, T., Harada, A., Miyamoto, N., Kawaguchi, T., Shimada, K., Ohkawa, S., Uemura, T., Yoshikawa, T., & Mori, E. (2008). Clinical impact of the callosal angle in the diagnosis of idiopathic normal pressure hydrocephalus. European radiology, 18(11), 2678–2683. https://doi.org/10.1007/s00330-008-1044-4
12. LeMay, M., & New, P. F. (1970). Radiological diagnosis of occult normal-pressure hydrocephalus. Radiology, 96(2), 347–358. https://doi.org/10.1148/96.2.347
13. Fällmar, D., Andersson, O., Kilander, L., Löwenmark, M., Nyholm, D., & Virhammar, J. (2021). Imaging features associated with idiopathic normal pressure hydrocephalus have high specificity even when comparing with vascular dementia and atypical parkinsonism. Fluids and barriers of the CNS, 18(1), 35. https://doi.org/10.1186/s12987-021-00270-3
14. Hashimoto, M., Ishikawa, M., Mori, E., Kuwana, N., & Study of INPH on neurological improvement (SINPHONI) (2010). Diagnosis of idiopathic normal pressure hydrocephalus is supported by MRI-based scheme: a prospective cohort study. Cerebrospinal fluid research, 7, 18. https://doi.org/10.1186/1743-8454-7-18
15. Virhammar, J., Laurell, K., Cesarini, K. G., & Larsson, E. M. (2014). Preoperative prognostic value of MRI findings in 108 patients with idiopathic normal pressure hydrocephalus. AJNR. American journal of neuroradiology, 35(12), 2311–2318. https://doi.org/10.3174/ajnr.A4046
16. Tans J. T. (1979). Differentiation of normal pressure hydrocephalus and cerebral atrophy by computed tomography and spinal infusion test. Journal of neurology, 222(2), 109–118. https://doi.org/10.1007/BF00313004
17. Holodny, A. I., Waxman, R., George, A. E., Rusinek, H., Kalnin, A. J., & de Leon, M. (1998). MR differential diagnosis of normal-pressure hydrocephalus and Alzheimer disease: significance of perihippocampal fissures. AJNR. American journal of neuroradiology, 19(5), 813–819.
18. Wardlaw, J. M., Smith, C., & Dichgans, M. (2013). Mechanisms of sporadic cerebral small vessel disease: insights from neuroimaging. The Lancet. Neurology, 12(5), 483–497. https://doi.org/10.1016/S1474-4422(13)70060-7
19. Poca, M. A., Mataró, M., Del Mar Matarín, M., Arikan, F., Junqué, C., & Sahuquillo, J. (2004). Is the placement of shunts in patients with idiopathic normal-pressure hydrocephalus worth the risk? Results of a study based on continuous monitoring of intracranial pressure. Journal of neurosurgery, 100(5), 855–866. https://doi.org/10.3171/jns.2004.100.5.0855
20. Bradley W. G., Jr (2015). CSF Flow in the Brain in the Context of Normal Pressure Hydrocephalus. AJNR. American journal of neuroradiology, 36(5), 831–838.https://doi.org/10.3174/ajnr.A4124
21. Ohara, S., Nagai, H., & Ueda, Y. (1989). CSF pulsatile flow on MRI and its relation to intracranial pressure. In J. T. Hoff & A. L. Betz (Eds.), Intracranial Pressure VII (pp. 410–415). Springer Berlin Heidelberg. https://doi.org/10.1007/978-3-642-73987-3_109
22. Bradley, W. G., Jr, Scalzo, D., Queralt, J., Nitz, W. N., Atkinson, D. J., & Wong, P. (1996). Normal-pressure hydrocephalus: evaluation with cerebrospinal fluid flow measurements at MR imaging. Radiology, 198(2), 523–529. https://doi.org/10.1148/radiology.198.2.8596861